

# Sphingosine kinase 1 mediates sexual dimorphism in fibrosis in a mouse model of NASH



David Montefusco<sup>1,\*</sup>, Maryam Jamil<sup>1</sup>, Melissa A. Maczys<sup>1</sup>, William Schroeder<sup>1</sup>, Moshe Levi<sup>2</sup>, Suman Ranjit<sup>2</sup>, Jeremy Allegood<sup>1</sup>, Dipankar Bandyopadhyay<sup>4</sup>, Reuben Retnam<sup>4</sup>, Sarah Spiegel<sup>1</sup>, L. Ashley Cowart<sup>1,3</sup>

## ABSTRACT

**Objective:** Men with non-alcoholic fatty liver disease (NAFLD) are more likely to progress to non-alcoholic steatohepatitis (NASH) and liver fibrosis than women. However, the underlying molecular mechanisms of this dimorphism is unclear. We have previously shown that mice with global deletion of SphK1, the enzyme that produces the bioactive sphingolipid metabolite sphingosine 1-phosphate (S1P), were protected from development of NASH. The aim of this study was to elucidate the role of hepatocyte-specific SphK1 in development of NASH and to compare its contribution to hepatoesteatosis in male and female mice.

**Methods:** We assessed mouse livers in early-stage fibrosis induced by high fat feeding, using single harmonic generation microscopy, LC-MS/MS analysis of hydroxyproline levels, and expression of fibrosis markers. We identified an antifibrotic intercellular signaling mechanism by culturing primary mouse hepatocytes alongside, and in co-culture with, LX2 hepatic stellate cells.

**Results:** We generated hepatocyte-specific SphK1 knockout mice (SphK1-hKO). Unlike the global knockout, SphK1-hKO male mice were not protected from diet-induced steatosis, inflammation, or fibrogenesis. In contrast, female SphK1-hKO mice were protected from inflammation. Surprisingly, however, in these female mice, there was a ~10-fold increase in the fibrosis markers Col1 $\alpha$ 1 and 2–3 fold induction of alpha smooth muscle actin and the pro-fibrotic chemokine CCL5. Because increased fibrosis in female SphK1-hKO mice occurred despite an attenuated inflammatory response, we investigated the crosstalk between hepatocytes and hepatic stellate cells, central players in fibrosis. We found that estrogen stimulated release of S1P from female hepatocytes preventing TGF $\beta$ -induced expression of Col1 $\alpha$ 1 in HSCs via S1PR3.

**Conclusions:** The results revealed a novel pathway of estrogen-mediated cross-talk between hepatocytes and HSCs that may contribute to sex differences in NAFLD through an anti-fibrogenic function of the S1P/S1PR3 axis. This pathway is susceptible to pharmacologic manipulation, which may lead to novel therapeutic strategies.

© 2022 The Authors. Published by Elsevier GmbH. This is an open access article under the CC BY-NC-ND license (<http://creativecommons.org/licenses/by-nc-nd/4.0/>).

**Keywords** Sphingolipid; Sphingosine-1-phosphate; Sphingosine kinase; Fibrosis; NASH; NAFLD

## 1. INTRODUCTION

Non-alcoholic fatty liver disease (NAFLD) encompasses a set of pathologies associated with ectopic lipid accumulation in hepatocytes [1]. NAFLD can progress to non-alcoholic steatohepatitis (NASH), an inflammatory condition which is increasing in prevalence in parallel with other diseases connected to lipid metabolism, such as type 2 diabetes and cardiovascular disease [2]. NASH is characterized by hepatic necrosis, increased inflammatory signaling, immune cell infiltration, and the potential to progress to fibrosis, cirrhosis, hepatocellular carcinoma, and ultimately liver failure [1,3,4].

Fibrosis is common to late stages of NAFLD, and if allowed to progress can lead to cirrhosis and loss of liver function [5]. Fibrosis is typically initiated by the release of pro-fibrotic cytokines such as TGF $\beta$  from several cell types including injured hepatocytes, resident immune cells, and infiltrating immune cells [6–10]. These cytokines activate

hepatic stellate cells and infiltrating bone marrow-derived stem cells in the liver sinusoids, where they deposit extracellular matrix proteins leading to fibrosis [11]. This straightforward and linear view of fibrosis is complicated, however, by observations that there are several pro-fibrotic and anti-fibrotic cytokines released by multiple cell types under different conditions [11].

There are several lines of evidence supporting that the female liver is protected from fibrosis; it is well documented that progression from NAFLD to NASH is more severe in men than in women, and that this discrepancy shrinks after menopause [12]. Furthermore, women following surgical menopause, or women with Turner's syndrome (i.e., lacking natural estrogen) have a higher risk of NAFLD [13]. The causes of this effect are complex, but estrogen has been proposed as a mediator of this protection. Estrogen [14] is known to be anti-fibrotic, and estrogen receptor agonists have been employed as anti-fibrotic therapeutics [15–18]. Due to the widespread physiologic

<sup>1</sup>Virginia Commonwealth University, Department of Biochemistry and Molecular Biology, VA, USA <sup>2</sup>Department of Biochemistry and Molecular & Cellular Biology, Georgetown University, USA <sup>3</sup>Hunter Holmes McGuire VAMC, Richmond, VA, USA <sup>4</sup>Virginia Commonwealth University Department of Biostatistics, VA, USA

\*Corresponding author. 2-016d Sanger Hall, 1101 E Marshall St., Richmond, VA 23298, USA. E-mail: [david.montefusco@vcuhealth.org](mailto:david.montefusco@vcuhealth.org) (D. Montefusco).

Received January 5, 2022 • Revision received May 4, 2022 • Accepted May 25, 2022 • Available online 6 June 2022

<https://doi.org/10.1016/j.molmet.2022.101523>

effects of these agonists [13], these approaches have led to potentially dangerous side effects, especially in mammary, uterine, and lung tissues [19–22]. In men, estrogen has been identified as a protective factor in NASH progression, however it is not in use in men as a therapeutic [23]. Therefore, pinpointing specific endogenous pathways by which estrogen mediates its anti-fibrotic effects has tremendous potential benefit if these pathways can be harnessed for therapeutic use.

Sphingosine kinase 1 (SphK1) generates the bioactive lipid sphingosine-1-phosphate (S1P), which serves as a ligand for a family of G protein-coupled receptors (S1PR1–5). SphK1 and S1P regulate pro-inflammatory responses and fibrosis in many organs and disease states [24–28]. Several studies have implicated SphK1 in NAFLD [29–35]. We showed that SphK1 is upregulated in human NASH and in livers from C57bl/6J mice fed HFD (60%kCal from milk fat) for 16 weeks [36]. This high saturated fat diet led not only to steatosis, but also caused hepatocyte ballooning, proinflammatory cytokine expression, immune cell infiltration, and histology consistent with human NASH. Moreover, these obese mice were insulin resistant and exhibited markers of ER stress in liver, indicating etiological and molecular overlap with human NASH. Using this model, we demonstrated that a constitutive SphK1-null mouse fed high saturated fat diet was protected from all aspects of NASH [36].

S1P is known to play a role in regulation of immune cells and the inflammatory response in a variety of diseases in multiple tissues and cell types [37–39]. In liver, SphK1 is expressed in several cell types, including resident macrophages, fibroblasts, endothelial cells, and hepatocytes [36,40]. Therefore, though liver triglyceride accumulation and inflammation were both attenuated in the SphK1 knockout [36], the role of SphK1 in hepatocytes was not known.

To examine a potential role for SphK1 specific to hepatocytes in the NASH development, we crossed SphK1-loxp/loxp mice [41] with Albumin:Cre (Alb-Cre) [42] mice yielding a hepatocyte-specific SphK1 null mouse (SphK1-hKO). As in humans, we observed notable sex differences between males and females in these mice fed the HFD. Most notably, female SphK1-hKO mice demonstrated a severely exacerbated upregulation of fibrosis markers including Col1 $\alpha$ 1, smooth muscle actin, and CCl5, and showed enhanced collagen deposition. Mechanistic studies indicated that estrogen stimulated release of S1P from female hepatocytes and that S1P prevented and also reversed expression of Col1 $\alpha$ 1 induced by TGF $\beta$  in HSCs, via S1PR3, which was induced upon HSC activation. These findings suggest a female-specific mechanism of suppressing fibrosis via estrogen dependent, S1P receptor-mediated cross-talk between hepatocytes and HSCs, which may contribute to sex differences observed in humans with NASH and could potentially be harnessed for treatment of fibrosis in males and post-menopausal women.

## 2. METHODS

### 2.1. Generation of the SphK1-hKO mouse

The Albumin Cre mouse was obtained from Jackson Laboratories, B6.Cg-Tg(Alb-cre)21Mgn/J stock number 003574. The SphK1 floxed mouse was obtained from the laboratory of Dr. Richard Proia (NIH). The mice were crossed by successive generations. Excision of the Sphk1 gene was confirmed by the forward primer 5'-GGACCTGGCTATGGAACC-3' and the reverse primer 5'-AATGCCTACTGCTTACAATAC-3', yielding a 300 bp product for the WT allele and a 600 bp product for the excised KO allele.

### 2.2. High fat diet

Mice were fed control or high fat diet ad libitum for 16 weeks. The control (TD.120455) and high fat (TD.09766) diets containing 6.2% and 34.3% fat by weight respectively, were obtained from Teklad.

### 2.3. Liver triglyceride levels

50 mg of tissue was dissolved in 6 $\times$  volume of 2:1 ethanol/30% KOH at 60 °C for ~5 h, vortexed periodically to improve digestion. A volume of 1.08 $\times$  the original volume of 1 M MgCl<sub>2</sub> was added, vortexed, and chilled on ice for 10 min. The digest was centrifuged at room temperature at 14,000  $\times g$  for 30 min, and supernatant was collected and diluted 1:10 in water for use in the triglyceride assay. The supernatant was measured with the Triglyceride LiquiColor Test (Stanbio 2200-225).

### 2.4. Gene expression by qPCR

Cells were harvested on ice by scraping into 0.2 ml Trizol per well, liver tissue was homogenized with a magnetic bead homogenizer in 1 ml of Trizol per 20 mg of tissue. RNA was extracted from Trizol using the Qiagen RNAeasy kit, and then reverse transcribed using the Biorad iScript kit. RNA quality of tissue samples was confirmed by bio-analyzer. A Sybr green protocol with a 58 °C annealing temperature for 40 cycles was used with primers listed in Table S1. Mean normalized expression was calculated by averaging beta actin and HMBS1 as the reference gene panel for mouse liver and hepatocytes, and beta actin for human LX2 cells. LX2 cells were obtained from Sigma/Millipore.

### 2.5. Western blotting

RIPA buffer containing Pierce protease and phosphatase inhibitors was added to liver tissues (50 mg/ml) or LX2 cells (0.2 ml per well). Liver samples were homogenized with a magnetic bead homogenizer, and cell or tissue proteins were quantified by BCA and prepared in 4 $\times$  Laemmli buffer at 2 mg/ml, and 15  $\mu$ g was loaded per well of a 26-lane 4–15% BioRad Criterion gradient gel. Membranes were blocked and blotted in 5% BSA in TBST. Human collagen 1 was blotted with the Cell Signaling antibody (84336) at 1:1000 dilution overnight at 4 °C. Cell Signaling anti-rabbit HRP secondary (7074S) was used as secondary antibody, blotted at 1:5000 at room temperature for 1 h.

### 2.6. Autofluorescence FLIM and SHG measurements using DIVER microscope

Second harmonic generation (SHG) signals were acquired using the DIVER (Deep Imaging Via Enhanced-Photon Recovery) detector originally developed at the Laboratory of Fluorescence Dynamics, University of California, Irvine, which is currently installed in the Microscopy Imaging Shared Resource at Georgetown University. A short pulsed two photon laser (Insight DeepSee X3, Spectra-Physics, Santa Clara, CA) adapted with an Acousto-Optic Modulator was used as the excitation source. The samples were viewed with a 10 $\times$  0.4NA air objective (Olympus, Waltham, MA), positioned directly on top of the DIVER detector assembly input window. Two-photon induced fluorescence signal was collected using a 410–460 nm band pass with an internal gallium arsenide phosphide large area photomultiplier tube (Hamamatsu R7600P-300, Bridgewater, NJ), with a modified UG11 glass filter (360–380 nm), and a FLIMBox (ISS, Champaign, IL). Signal was converted to a phasor plot [43], with rhodamine 110 (lifetime = 4.0 ns) used for the phasor plot calibration. Each SHG image was taken with a 1250  $\mu$ m field of view, 20  $\mu$ s pixel dwell time and 16 repeat scans with 256  $\times$  256 pixels/image. SHG and fluorescence images were collected simultaneously after excitation with a

740 nm laser line. The data collection and analysis were carried out by using SimFCS. SHG appears at  $S = 0$ ,  $G = 1$  in the phasor plot and is selected using a circular green cursor (Figure 3C) [44–46].

### 2.7. Culture of LX2 stellate cell line

LX2 cells were purchased from Sigma (SCC064) and cultured in High Glucose DMEM with 2% FBS with Pen/Strep and L-glutamine.

### 2.8. Isolation of primary mouse hepatocytes

Isolation was carried out based on the method of Seglen et al. [47]. Briefly, the inferior vena cava (IVC) was catheterized under isoflurane anesthesia, the IVC was clamped anterior to the heart, and then the liver was flushed from the portal vein with heparin, then EGTA perfusate, and then collagenase perfusate. Hepatocytes were isolated by Percoll gradient and cultured in supplemented William's E media (Gibco).

### 2.9. Hepatocyte-stellate co-culture experiments

LX2 stellate cells were plated on Costar polystyrene transwells with a 0.4  $\mu\text{m}$  pore size at  $3 \times 10^5$  cells per well. LX2 cells were starved in serum-free DMEM containing 0.2% fatty-acid-free BSA and Pen/Strep at time zero ( $t = 0$ ). Hepatocytes were isolated from female C57/Bl6 wild type, or SphK1 global constitutive knockout mice [36], and plated on 6 well dishes at  $3 \times 10^5$  cells per well. Hepatocytes were then pre-treated for 12 h with 17 $\beta$ -estradiol (E2) or vehicle (0.005% ethanol) in DMEM with 10% FBS and Pen/Strep at  $t = 36$  h. At  $t = 48$  h, media was aspirated from both cell types and replaced with LX2 starvation media with or without 2.5 ng/ $\mu\text{l}$  TGF $\beta$ , and then LX2-containing transwells were placed into hepatocyte-containing 6-well dishes. At  $t = 60$  h, LX2 cells were harvested into Trizol for RNA extraction.

### 2.10. Cell treatments

Cells were treated with S1P (Avanti Polar Lipids 860492), 17 $\beta$ -Estradiolestradiol (Sigma E8875), or human recombinant TGF $\beta$  (R&D Biosystems 7754-BH-005). S1P was suspended in LX2 starvation media containing 0.4% fatty-acid-free BSA and solubilized in a bath sonicator. HS173 and receptor antagonists TY52156, and W146 were obtained from (Cayman Chemicals) and delivered in 0.05% DMSO, JTE-13 was obtained from Sigma.

### 2.11. Hydroxyproline measurements

Hydroxyproline was measured by LC–MS based on a published method [48] using a deuterated hydroxyproline internal standard (CDN isotopes, cis-4-hydroxy-L-proline-2,5,5-d $_3$ , d-7713, mw = 134.15). Hydroxyproline was liberated from collagen by acid hydrolysis. 10 mg of tissue was homogenized by an immersion blender into 100  $\mu\text{l}$  of water. 100  $\mu\text{l}$  of homogenate was placed in a Teflon-lined screw top glass test tube and 100  $\mu\text{l}$  of 12 N HCl was added. The tube was capped and heated for 3 h at 120  $^{\circ}\text{C}$ . After cooling to RT, 120  $\mu\text{l}$  of 10 N NaOH, and 5 mg of activated charcoal was added. Samples were vortexed and centrifuged at  $10,000 \times g$  for 5 min. Sample volumes were equalized to 260  $\mu\text{l}$  with H $_2$ O, and a 60  $\mu\text{l}$  aliquot was removed for BCA assay. The remaining solution was transferred to a clean glass tube, dried under nitrogen and resuspended in mobile phase. For LC–MS, hydroxyproline was separated in a fixed mobile phase of 5% CH $_3$ CN with 10 mM CH $_3$ COONH $_4$  in a 150  $\times$  2 mm C-18 column at 0.2 ml/min and the 131.15 M+ peak was quantified.

### 2.12. CCl $_4$ -induced fibrosis

10-week-old mice were injected with 1  $\mu\text{l}$  CCl $_4$  per gram of body weight (Sigma 289116), diluted 1 to 3 in corn oil (Kroger, pure corn oil), twice per week for 6 weeks.

### 2.13. Measurement of S1P by LC–ESI-MS/MS

Hepatocytes from WT and SphK1-hKO mice cultured in 6-well tissue culture plates were washed with PBS and treated with vehicle or E2 (100 nM) in medium containing 1% FA-free BSA for the indicated times. Plates were then placed on ice, and the medium was removed and added to prechilled 13  $\times$  100 mm borosilicate tubes containing 1 ml of ice-cold methanol. Cells were washed with PBS and 300  $\mu\text{l}$  of ice cold-PBS containing 1:100 HALT protease, and phosphatase inhibitor was added. Cells were scraped, and suspensions (200  $\mu\text{l}$ ) were added to 13  $\times$  100 mm borosilicate tubes containing 0.5 ml of methanol. An aliquot of the remaining 100  $\mu\text{l}$  cell suspension was used for protein quantification. Sphingolipids were measured by LC–ESI-MS/MS (Sciex 5500 QTRAP; ABSciex, Farmingham, MA) as previously described [49]. Cellular sphingolipid levels were expressed as pmol per milligram of protein and secreted as pmol per milliliter of medium.

### 2.14. Statistics

P-values where indicated were generated by a 2-tailed Student's t-test, or one way ANOVA followed by Dunnett's multiple comparisons test, where multiple groups were present. Mouse weight data was fit with a linear mixed model with 8 groups defined by combinations of gender, mutation, and diet and interactions of these groups with weeks. P-values for estimated differences in slope were corrected for multiple testing via Tukey correction.

#### 2.14.1. Approval of animal studies

All animal experiments conformed to the National Institutes of Health Guide for the Care and Use of Laboratory Animals and were in accordance with Public Health Service/National Institutes of Health guidelines for laboratory animal usage. The experimental groups consisted of male and female WT and SphK1-hKO C57BL/6 mice. Mice were housed in the animal facility at the Medical University of South Carolina and Virginia Commonwealth University. Food and water were provided ad libitum, animals were maintained on a 12:12 h light–dark cycle and ambient temperature was steadily 21  $^{\circ}\text{C}$ . Animals were randomized to a high saturated fat diet (HFD) (Envigo, TD.09766) (60% kcal provided by milkfat) or an isocaloric low-fat diet (CD) (Envigo, TD.120455) (17% kcal provided by lard) at 10 weeks of age, and diets were administered for 16 weeks ( $n = 5$  per group). Mice were euthanized humanely by isoflurane (Hospira, Inc., Lake Forest, IL) followed by cardiac puncture. Cardiac blood was prepared for nonhemolyzed serum, aliquoted, and stored at  $-80^{\circ}\text{C}$ . Tissues were collected accordingly as fresh fixed in 10% neutral buffered formalin or fresh snap-frozen in liquid nitrogen and stored at  $-80^{\circ}\text{C}$ . All study methods were approved by the IACUC boards of the Medical University of South Carolina, and Virginia Commonwealth University where phases of the study were completed.

## 3. RESULTS

### 3.1. Hepatocyte-specific depletion of sphingosine kinase 1

Previous work employing the global SphK1 knockout revealed that expression of TNF $\alpha$ , MCP1, and phosphorylation of IK $\beta$  $\alpha$  induced by high fat feeding were attenuated in the knockout mice [36]. Because hepatocytes comprise 70–80% of cells in liver and are central to liver injury and progression of inflammation, it was hypothesized that protection from NASH observed in the global knockout was driven by hepatocyte SphK1 expression. Thus a hepatocyte-specific SphK1 knockout mouse was generated by crossing the SphK1-flox/flox mouse with albumin-Cre [50]. We confirmed gene depletion in the liver tissue genome by qPCR (Figure S1C). While chow-fed mice expressed SphK1, expression was severely attenuated in liver homogenates from

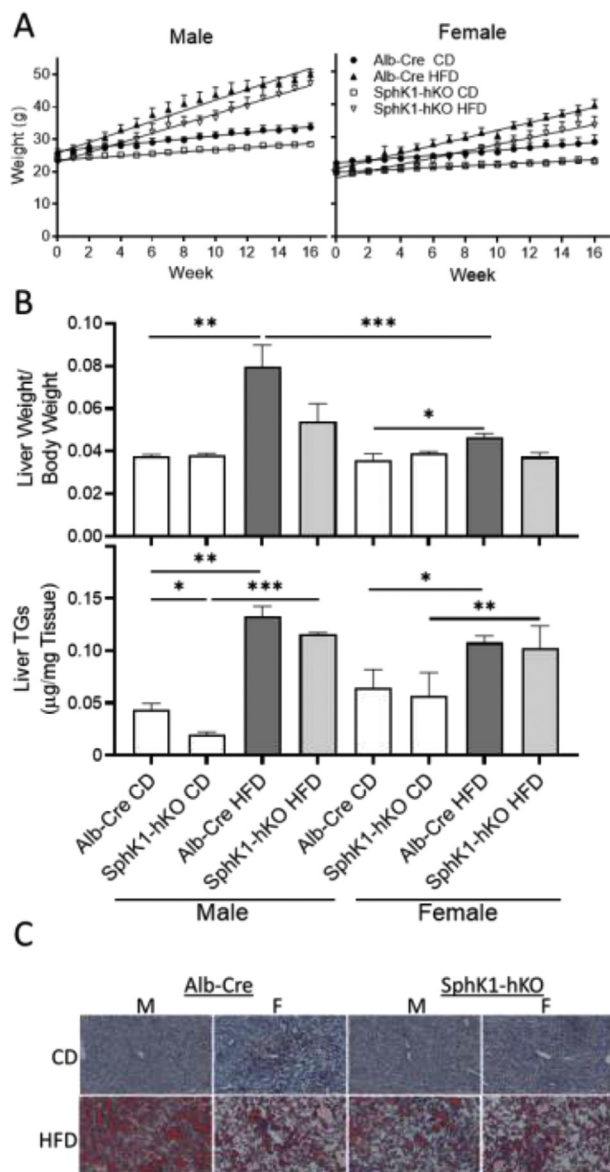


**Figure 1: Weight gain, tissue weight, and liver TGs of high fat diet fed mice.** 10-week-old chow-fed mice were fed a high saturated fat milk fat-based diet (HFD) or low glycemic control diet (CD) until 26 weeks of age. (A) Weight gain in wild type (Alb-Cre) and hepatocyte-specific sphingosine kinase knockout (SphK1-hKO) mice. Mouse weight data was fitted to a Linear Mixed Model to determine if weight gain differed significantly between sex and genotype, and the fit parameters are listed in Table 1. (B) The ratio of liver weight to body weight and triglyceride content per weight of tissue, as measures of hepatomegaly and steatosis, respectively. (C) Lipid droplet deposition for HFD and CD mice was examined by neutral lipid staining with Oil Red O. N = 5, error bars are SEM, significance between diet, sex and genotype comparisons was identified by one way ANOVA followed by Dunnett's multiple comparisons test P < \*0.05, \*\*0.01, \*\*\*0.001.

SphK1-hKO mice, not only indicating sufficient activity of the Alb-CRE/flox depletion system but also suggesting that hepatocytes are the primary source of SphK1 mRNA in liver.

### 3.2. The SphK1-hKO mouse is partially protected from liver weight gain, but not TG accumulation

Both male and female Alb-Cre and SphK1-hKO were fed high saturated fat diet (HFD) or control diet (CD) for 16 weeks starting at 10 weeks of age. HFD led to profound weight gain relative to CD, which was

comparable in males and females (Figure 1A). Though SphK1-hKO mice of both sexes trended toward reduced weight gain, the differences were not significant (Table 1). Hepatomegaly, represented by increased liver weight with HFD relative to total body weight, is common with the development of NASH, and both male and female SphK1-hKO mice were protected from hepatomegaly, which was not accompanied by a proportional decrease in TG accumulation (Figure 1B). TGs were significantly increased with HFD in both the wild type and SphK1-hKO mice. Oil red O staining of liver sections indicated a similar degree of steatosis in both male female wild type and SphK1-hKO mice (Figure 1C).

### 3.3. The SphK1-hKO mouse was partially protected from diet-induced inflammation

HFD-induced expression of the proinflammatory cytokines TNF $\alpha$  and MCP1 and also immune cell infiltration were attenuated in the global SphK1 knockout mice [36]. In contrast, inflammatory responses were not reduced in male SphK1-hKO mice. However, female SphK1-hKO mice were protected from increased inflammation, suggesting a different function of SphK1 in male vs. female hepatocytes. Specifically, both TNF $\alpha$  and MCP1 increased significantly in Alb-Cre mice fed HFD compared to CD but they were not increased in SphK1-hKO females. Similarly, expression of the cytokine CXCL10 involved in the development of NASH, was significantly lower in SphK1-hKO females than in Alb-Cre females both on CD and with high fat feeding, implying that hepatocyte SphK1 is at least partially responsible for inducing inflammation in females (Figure 2).

### 3.4. Exacerbation of diet-induced upregulation of fibrosis in female SphK1-hKO female mice

A common cause of patient mortality associated with fatty liver disease is cirrhosis, which is preceded by increased cell damage and death leading to progressive fibrosis [51]. While markers of inflammation and cell damage emerge early in mice with high fat feeding, the extensive cell damage associated fibrosis seen in patients is difficult to fully model in a rodent diet study. Thus, we examined early-emerging markers of NASH-associated fibrosis including collagen1 $\alpha$ 1 (Col1 $\alpha$ 1), smooth muscle actin ( $\alpha$ SMA) and the pro-fibrotic chemokine ligand 5 (CCL5), which was shown to be secreted by HSCs [52]. In male mice, Col1 $\alpha$ 1 expression increased in the WT mice fed HFD and was attenuated in SphK1-hKO mice (Figure 3A), while  $\alpha$ SMA and CCL5, trended up in male HFD fed mice, but did not reach statistical significance. However, while expression of Col1 $\alpha$ 1,  $\alpha$ SMA, and CCL5 did not change with diet in wild type females, female SphK1-hKO mice responded to the HFD with a striking ~10-fold increase in Col1 $\alpha$ 1 and 2–3-fold increase in  $\alpha$ SMA and CCL5 expression. To examine the level of collagen protein in NASH liver tissue, hydroxyproline, a modified form of proline that is nearly exclusive to collagen, was measured by LC-MS/MS (Figure 3B). Like the levels of collagen mRNA, the female knockout mice had significantly higher levels than both wild type controls and male knockouts. Comparing Alb-Cre HFD male to female, Col $\alpha$ 1 expression is slightly lower in females, while HP levels are higher in females. These not significantly significant, but we suspect this pattern is due at least in part to the stability difference between mRNA, and collagen protein, which is particularly long-lived.

To establish the severity of the fibrosis phenotype, second harmonic generation microscopy (SHG) was carried out on whole unstained tissue sections (Figure 4D). SHG is sensitive to molecules that are non-centrosymmetric, such as collagen fibers [53]. Specific signals from SHG were selected using the phasor approach to fluorescence lifetime imaging as SHG signal is coherent and has a lifetime of zero and

**Table 1** — Fit parameters for mouse weight gain.

Group 1	Group 1 slope (g/week, 95% CI)	Group 2	P-value, group 1 vs. 2
CD Alb-Cre male	0.511 (0.281–0.741)	HFD Alb-Cre male	<0.001
—	—	CD SphK1-hKO male	0.875
—	—	CD Alb-Cre female	0.997
CD Alb-Cre female	0.395 (0.165–0.625)	HFD Alb-Cre female	<0.001
—	—	CD SphK1-hKO female	0.967
HFD Alb-Cre male	1.591 (1.361–1.821)	HFD SphK1-hKO male	>0.999
—	—	HFD Alb-Cre female	0.133
HFD Alb-Cre female	1.149 (0.919–1.379)	HFD SphK1-hKO female	0.993
CD SphK1-hKO male	0.286 (0.056–0.516)	HFD SphK1-hKO male	<0.001
—	—	CD SphK1-hKO female	<0.001
CD SphK1-hKO female	0.222 (–0.008–0.452)	HFD SphK1-hKO female	<0.001
HFD SphK1-hKO male	1.517 (1.287–1.747)	HFD SphK1-hKO female	0.054
HFD SphK1-hKO female	1.017 (0.787–1.247)	—	—

appears at  $S = 0$ ,  $G = 1$  of the phasor plot (Figure 4C), [44–46,54]. The level of signal for HFD animals is similar for male and female Alb-Cre as well as male SphK1-hKO, however female SphK1-hKO mice revealed striking higher extent of collagen deposition. The Alb-Cre and SphK1-hKO male images showed very modest fibrosis, still at the F0 METAVIR grade [55,56], whereas female tissues were in the F1 grade, showing the early stages of bona fide fibrosis, with thickening bands of collagen deposited around the central veins and an emerging chicken-wire pattern in the more affected areas.

### 3.5. Sphingosine-1-phosphate decreased TGF $\beta$ -induced expression of Col1 $\alpha$ 1

In NAFLD, resident hepatic stellate cells (HSCs) are activated from a non-proliferative, quiescent state to secrete collagen and other pro-fibrotic factors [10]. Thus, the exacerbation of Col1 $\alpha$ 1 upon depletion of hepatocyte SphK1 suggests cross-talk between hepatocytes and HSCs. It seemed likely that this could be mediated by the paracrine actions of S1P that occur via signaling through a family of S1PRs. To test this, LX2 human HSCs were activated by treatment with TGF $\beta$  (an inducer of fibrogenesis and Col1 $\alpha$ 1 expression), and S1PR expression was assessed by qPCR. Strikingly, upon activation of LX2 cells, there was a 2–2.5-fold induction of S1PR3 expression, (Figure 4A).

Next, Col1 $\alpha$ 1 was selected as a marker to evaluate the action of S1P, because it showed a robust  $\sim$ 10-fold increase with HFD SphK1-hKO females, versus 2–3 fold for SMactin and CCl5 (Figure 3). To determine whether S1P could inhibit collagen expression in a paracrine-dependent manner, TGF $\beta$ -activated LX2 stellate cells were treated with S1P. S1P treatment significantly decreased the TGF $\beta$ -induced upregulation of Col1 $\alpha$ 1 mRNA (Figure 4B) and protein (Figure 4C), implying that binding of S1P to cell surface S1PRs may repress stellate cell activation. Maximum inhibition was observed at a concentration around 100 nM S1P (Figure 4D), which is within the physiological concentration range of S1P and consistent with the  $K_d$  of S1PRs for S1P [57]. Furthermore, collagen levels were evaluated in activated LX2 cells treated with S1P in the presence of S1P receptor antagonists targeting S1PR1, 2, or 3. While S1PR1 and 2 antagonists did not affect S1P-mediated collagen inhibition, in contrast, the S1PR3 antagonist reversed the S1P-dependent decrease in collagen (Figure 4E).

### 3.6. Estrogen increases secretion of S1P from hepatocytes

Estrogen has been shown to have antifibrotic effects in several liver diseases [13]. Because the collagen deposition observed in the female HFD fed mice appeared to be independent of inflammatory pathways (which were suppressed in female mice by SphK1 depletion), and estrogen was shown to activate SphK1 [49,58], we hypothesized that

estrogen may suppress fibrosis in HFD fed female mice by activating SphK1 and increasing its product S1P. To test this, WT or SphK1 deleted primary hepatocytes were treated without or with the major active estrogen, 17 $\beta$  estradiol (E2), for 12 h. Cells were thoroughly washed and media and replaced with TGF $\beta$  containing media. These hepatocytes were then co-cultured with LX2 stellate cells using transwell dishes for an additional 12 h (Figure 4F). Col1 $\alpha$ 1 upregulation by TGF $\beta$  in LX2 cells was suppressed by E2-treated WT hepatocytes, but not by SphK1 deleted hepatocytes (Fig 4G). While there are reports of direct action of E2 on HSCs [59,60], it should be noted LX2 cells were not directly exposed to E2 in this experiment, but rather only exposed to material secreted by hepatocytes following pre-treatment with E2, as well as exogenous TGF $\beta$  [21,61]. To test the possibility that E2 treatment induced release of S1P from hepatocytes, hepatocytes were treated with E2, and S1P levels were quantified in cells and in the media by LC–ESI-MS/MS. S1P appeared in the media at 30–120 min following E2 treatment, and this increase was significantly attenuated in SphK1–/– hepatocytes (Figure 4H). Additionally, S1P levels were significantly lower in SphK1–/– hepatocytes (Figure 4J). Male wild type hepatocytes were also subjected to E2 treatment to establish that this effect is sex-specific. Levels of S1P in the media of male hepatocytes was very low, and was not altered by E2 (Figure 4I), and levels in male hepatocytes were found to be higher than females, and also unaffected by E2 (Figure 4K). Taken together, our results suggest that E2 stimulates S1P release from female hepatocytes, which in turn activates S1PR3 on stellate cells to suppress collagen deposition.

## 4. DISCUSSION

In this study, we show that loss of SphK1 in murine hepatocytes dramatically exacerbated expression and deposition of liver collagen in NAFLD in a highly sex-dependent manner. Moreover, our data suggest an estrogen-mediated fibrosis-suppressing/reversing function for SphK1; however, the dominant view in the literature on the relationship between SphK1, S1P, and liver fibrosis is that increased SphK1/S1P contributes to fibrosis [62]. Indeed, elevated S1P has been shown in biopsies of patients suffering from fibrosis, as well as in common rodent models of fibrosis induced by bile duct ligation, CCl<sub>4</sub>, and methionine choline deficient diet [40,63,64]. Furthermore, circulating [40,65] S1P correlated with advanced disease and increased SphK1 expression [24,40,63,64]. A pro-fibrotic role for SphK1/S1P is also supported by several in vivo studies. For example, the S1PR2 knockout mouse [66,67] and the SphK1–/– mouse [36] are protected from fibrosis, and S1PR antagonists have been shown to protect against fibrosis in some cases [23,68–70]. These data point to a generalized

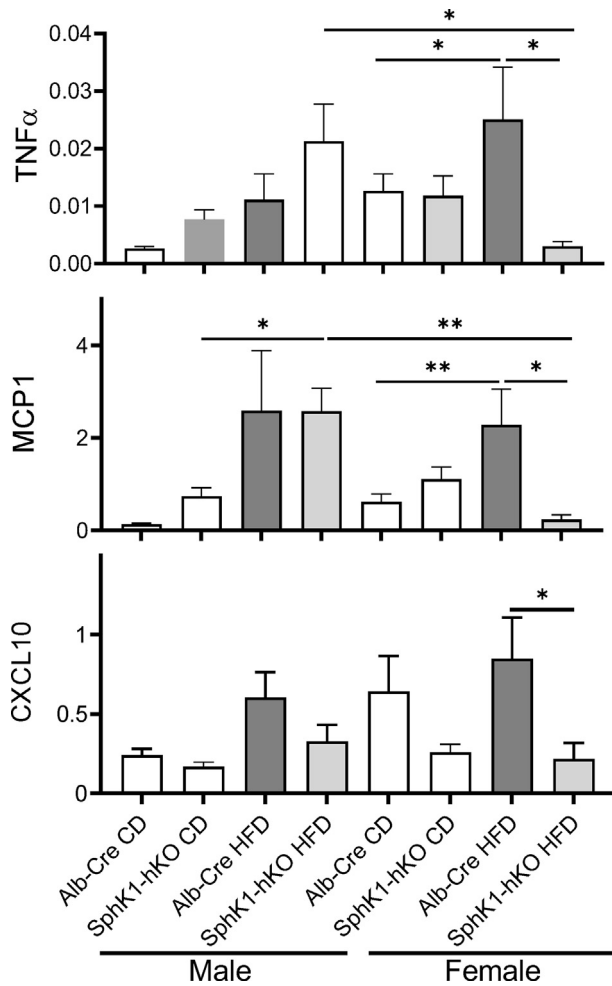


**Figure 2: Effect of high fat diet feeding on key inflammatory markers in the liver.** Expression of inflammatory markers TNF $\alpha$ , MCP1 and CXCL10 in wild type mice (Alb-Cre) hepatocyte-specific SphK1 knockout (SphK1-hKO) strain with high fat diet (HFD) versus control diet (CD). Wild type and SphK1-hKO mice were fed high saturated fat diet for 16 weeks. RNA was extracted from liver, reverse transcribed and analyzed by qPCR. Beta actin and Hmbs1 were averaged as a reference gene panel. N = 5, error bars are SEM. Significance between diet, sex, and genotype was determined by one way ANOVA followed by Dunnett's multiple comparisons test P < \*0.05, \*\*0.01.

association of S1P with increased fibrosis. Contrastingly, in a liver regeneration model, S1P promoted liver regeneration leading to indirect but dramatic inhibition of fibrosis [71]. However, while increased S1P in the liver, and even in circulation, is associated with fibrosis, the pathways giving rise to fibrosis are highly complex.

Much of the complexity in the emergence of liver fibrosis arises from the involvement of multiple cell types, but the central players in production of fibrotic tissue are HSCs. Roles for SphK1/S1P/S1PR signaling have been identified in HSCs, although they are all in the context of TGF $\beta$ -induced SphK1 transcription and activation in the HSC, as opposed to S1P originating from other cell types. SphK1 activity in HSCs induced by TGF $\beta$  pathway was implicated in transcription of fibrosis markers [72], and the reported point of action varies [73], but according to Kageyama et al. and Brunati et al. [70,74], S1PR2 expressed by HSCs was identified as the target, and upregulation of S1PR2 was required. There is no evidence of activation of HSCs by exogenous S1P, and in fact, an attempt to establish activation by a direct interaction showed the opposite [75]. Moreover, it has been

suggested that TGF $\beta$ -induced intracellular S1P contributes to collagen expression in hepatic myofibroblasts, independent of S1PRs [76]. Hence, it is tempting to speculate that activation of HCS by exogenous S1P has the opposite effects on fibrosis than those induced by intracellular S1P produced by TGF $\beta$ -mediated activation of SphK1. Here we show that physiological levels of E2 induce release of S1P from female hepatocytes but not from male hepatocytes. S1P release was significantly lower in SphK1 $^{-/-}$  hepatocytes compared to WT. We are presenting a novel mechanism that hepatocyte-derived SphK1/S1P links estrogen signaling to suppression of liver fibrosis (Fig 4J). There is little supporting literature linking these processes in liver, though it is well established that estrogen activates SphK1 leading to production of S1P in other cell types [77]. S1P and estrogen signaling, however, have been linked indirectly in a liver fibrosis context through the lipoprotein-bound S1P, and estrogen was reported to induce hepatic secretion of ApoM [78]. Furthermore, overexpression of ApoM was shown to cause a

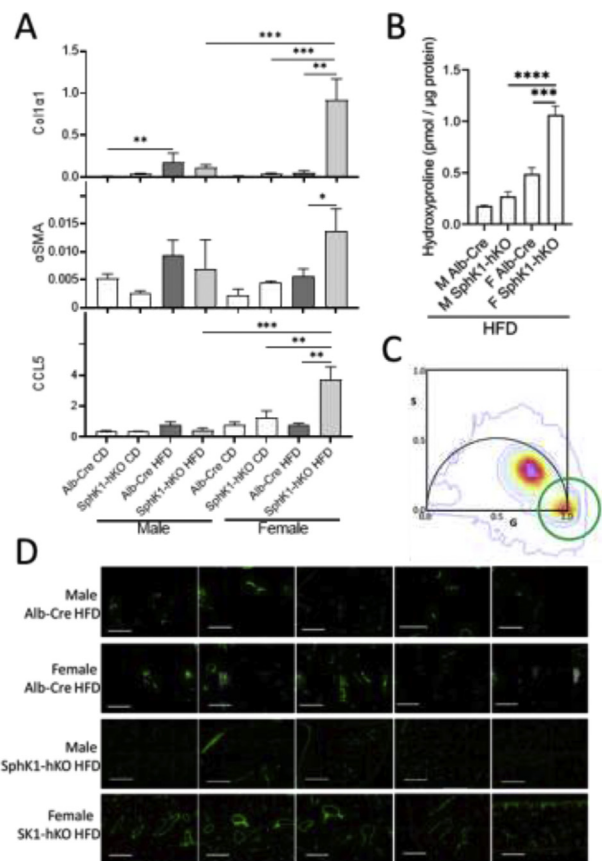


**Figure 3: Assessment of liver fibrosis.** (A) Upregulation of early fibrosis markers collagen1 $\alpha$ 1 (Col1 $\alpha$ 1), alpha smooth muscle actin (SMactin) and CCL5 mRNA with high fat diet (HFD). Col1 $\alpha$ 1,  $\alpha$ SMA, and CCL5 expression in liver homogenate by qPCR, for wild type (Alb-Cre) and SphK1-hKO for control diet (CD) and high fat diet (HFD) groups, beta actin and Hmbs1 were averaged as a reference gene panel. (B) Hydroxyproline was quantified in liver tissue from high fat diet (HFD) male (M) and female (F) mice by LC-MS/MS, as a proxy for total collagen levels. (D) Unstained paraffin-embedded liver sections from HFD mice were imaged using Second Harmonic Generation (SHG) microscopy, scale bar = 700  $\mu$ m. (C) SHG signal was selected based on the lifetime of zero which has a phasor signature of G = 1, S = 0 (green circle). Significance between diet, sex and genotype comparisons was identified by one way ANOVA followed by Dunnett's multiple comparisons test N = 5, error bars are SEM, P < \*0.05, \*\*0.01, \*\*\*0.001, \*\*\*\*0.0001.

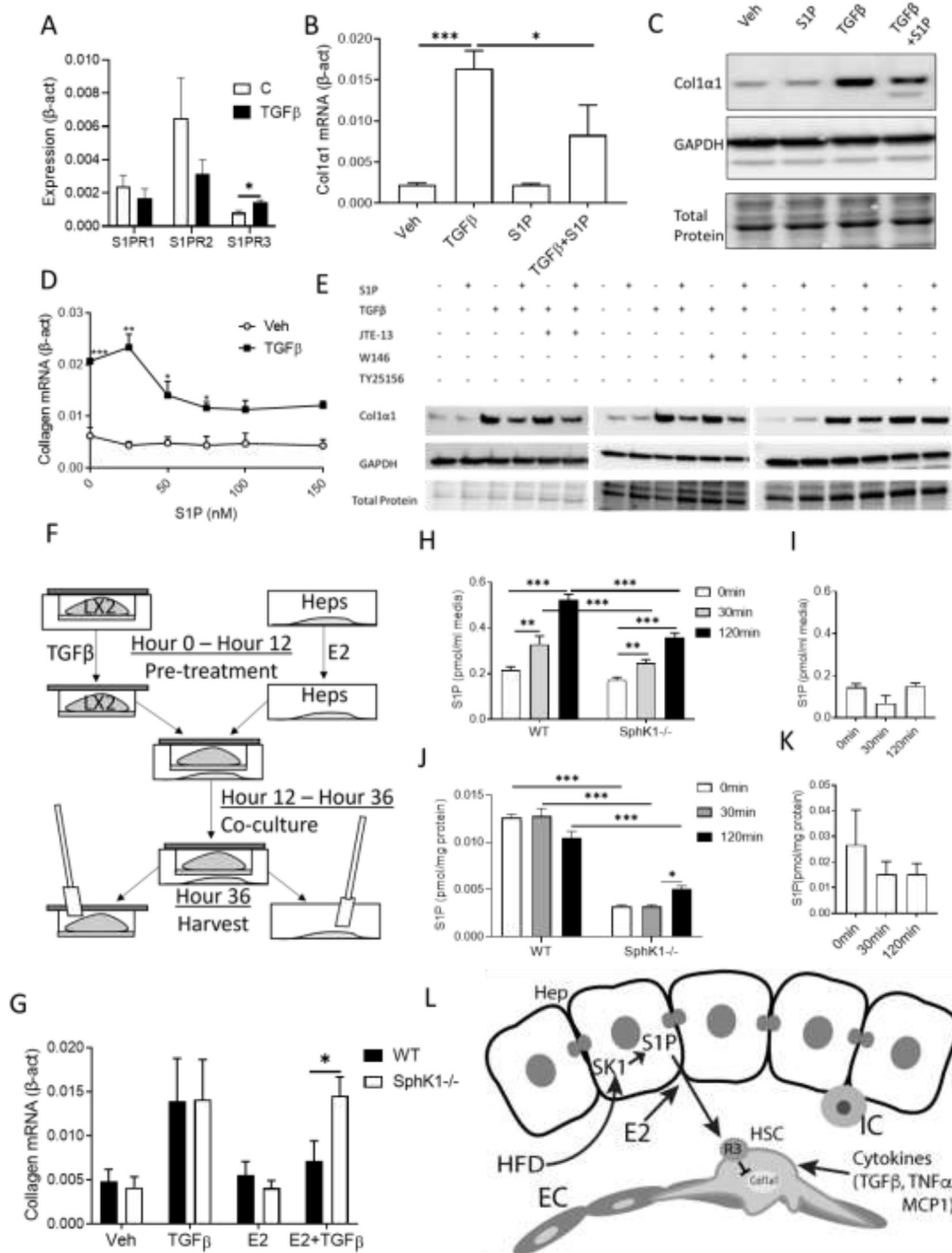


**Figure 4: Hepatocyte-Derived S1P suppress collagen expression in LX2 Hepatic stellate cells via S1PR3.** (A) S1P mRNA expression in TGFβ activated LX2 cells (N = 7), for all qPCR data presented for LX2 cell, beta actin was used as the reference gene. (B–D) Col1α1 expression in LX2 hepatic stellate cells, pre-activated by TGFβ alone for 18 h and then treated with vehicle (Veh), TGFβ (2.5 ng/ml), S1P, or TGFβ + S1P for an additional 6 h. (B) QPCR or (C) Western blot show TGFβ-induced expression of collagen in hepatic stellate cells suppressed by treatment with 100 nM S1P. (D) Inhibition of Col1α1 expression by S1P was dose dependent with a maximal effect achieved at 100 nM (N = 3). (E) Cells treated with TGFβ (2.5 ng/ml), S1P (100 nM), S1PR1 and 2 antagonists JTE-13 and W146 respectively (1 μM), and S1PR3 antagonist TY25156 (1 μM). Western blots are representative of biological triplicates. (F,G) Hepatocyte-derived S1P suppresses collagen induction in a hepatocyte-HSC co-culture model described in the schematic (F). LX2 cells were cultured in transwells until confluent, primary hepatocytes (Heps) were plated onto collagen-coated 6 well dishes. At hour 0, LX2 cells were treated with vehicle (Veh) or TGFβ (2.5 ng/ml), and hepatocytes with vehicle or 17β-estradiol (E2, 100 nM) for 12 h. Following pre-treatment, transwells containing LX2 cells were placed into 6 well dishes containing hepatocytes, TGFβ or E2 were removed, and fresh media was applied. Following 12 h of co-culture, LX2 cells were harvested. (G) Col1α1 expression in LX2 hepatic stellate cells co-cultured with primary hepatocytes isolated from wild type (WT) or sphingosine kinase knockout mice (SphK1<sup>-/-</sup>) on transwell dishes (N = 6). Primary hepatocytes isolated from male and female mice were treated with 100 nM 17β-estradiol. S1P levels secreted into the media was measured for female (H) and male (I) hepatocytes, as well as in cells for female (J) and male (K) by LC-ESI-MS/MS (N = 3). (L) High fat diet (HFD) causes injury in hepatocytes (Hep) and endothelial cells (EC) inducing pro-inflammatory S1P signaling in immune cells (IC) leading to indirect activation of hepatic stellate cells (HSC). S1P inhibits collagen (Col1α1) expression in HSC through S1PR3, opposing TGFβ-driven activation. Error bars are SEM, Student's t-test P < \*0.05, \*\*0.01, \*\*\*0.001.

dramatic increase in hepatic S1P secretion [79]. While it is unknown whether the effects on HSCs require ApoM or the ApoM receptor, it is known that albumin-bound versus ApoM-bound S1P can have differential effects [80,81]. Interestingly, a study found that female type 1 diabetes patients, but not male, had elevated ApoM and S1P in their light HDL fraction [47], suggesting that secretion of hepatic S1P in response to the disease occurred only in women. However, it should be reiterated, that in our model system we showed S1P inhibition of Col1 $\alpha$ 1 expression in LX2 HSCs in the absence of ApoM. Our study reveals potential deleterious effects of targeting hepatic SphK1 activity as a therapeutic strategy, especially in female patients, and raises the possibility of exploiting S1P signaling to reverse fibrosis in both female and male patients by targeting HSCs directly via S1PR3 activation.

### AUTHOR CONTRIBUTIONS

DM and LAC conceived of and directed the project. DM carried out the animal study and collected much of the in vivo data. DM and MJ carried out co-culture experiments and other experiments in hepatic stellate cells. MM designed and performed the experiments on S1P release in primary hepatocytes under the supervision of SS. PR collected a significant amount of in vivo data and assisted with critical tissue collection. WS collected protein expression data and assisted with quantification of microscopy images. WH collected gene expression data. SS provided intellectual contribution in the realm of S1P, liver pathology, inflammation and fibrosis. RR performed statistical analyses, DB provide expertise in statistical analysis AS provided intellectual contribution in the realm of liver pathobiology, inflammation and fibrosis. LAC provided a major intellectual contribution in the role of SPHK1 and S1P in liver pathology, inflammation and fibrosis. DM and LAC wrote the manuscript. ML provided expertise on SHG microscopy. SR Provided expertise on, and collected and analyzed, SHG microscopy images.

### ACKNOWLEDGMENTS

We would like to acknowledge members of the Cowart lab including Andrea Anderson and Johanna Lambert as well as members of the Spiegel lab including Dr. Jason Newton. We would like to acknowledge the VCU lipidomics core, and Massey Cancer Center Histology Core. Department of Veterans Affairs 210BX00200-04, National Institutes of Health 1R01HL117233 and 1R01HL151243 (LAC), the McGuire Research Institute and Virginia Commonwealth University joint pilot program (DM), Centers of Biomedical Research Excellence in Lipidomics & Pathobiology 5P30GM103339-03 and the Massey Center Cancer Support Grant P30 CA016059-39. SS was supported by R01GM043880. We would like to acknowledge Microscopy and Imaging Shared Resource (MISR), the VCU Biostatistic Shared Resource, for the instrumentation to acquire SHG images.

### CONFLICTS OF INTEREST

The authors have no conflicts of interest to declare.

### APPENDIX A. SUPPLEMENTARY DATA

Supplementary data to this article can be found online at <https://doi.org/10.1016/j.molmet.2022.101523>.

### REFERENCES

- [1] Kim, H., Lee, D.S., An, T.H., Park, H.J., Kim, W.K., Bae, K.H., et al., 2021. Metabolic spectrum of liver failure in type 2 diabetes and obesity: from nafld to

- nash to hcc. *International Journal of Molecular Sciences* 4495. <https://doi.org/10.3390/ijms22094495>.
- [2] Jichitu, A., Bungau, S., Stanescu, A.M.A., Vesa, C.M., Toma, M.M., Bustea, C., et al., 2021. Non-alcoholic fatty liver disease and cardiovascular comorbidities: pathophysiological links, diagnosis, and therapeutic management. *Diagnostics* 11(4):689. <https://doi.org/10.3390/diagnostics11040689>.
- [3] Stefan, N., Haring, H.-U., Cusi, K., 2019. Non-alcoholic fatty liver disease: causes, diagnosis, cardiometabolic consequences, and treatment strategies. *The Lancet. Diabetes & Endocrinology* 7(4):313–324. [https://doi.org/10.1016/S2213-8587\(18\)30154-2](https://doi.org/10.1016/S2213-8587(18)30154-2).
- [4] Schattenberg, J.M., Schuppan, D., 2011. Nonalcoholic steatohepatitis: the therapeutic challenge of a global epidemic. *Current Opinion in Lipidology* 22(6): 479–488. <https://doi.org/10.1097/MOL.0B013E32834C7CFC>.
- [5] Heyens, L.J.M., Busschots, D., Koek, G.H., Robaey, G., Francque, S., 2021. Liver fibrosis in non-alcoholic fatty liver disease: from liver biopsy to non-invasive biomarkers in diagnosis and treatment. *Frontiers of Medicine* 8: 615978. <https://doi.org/10.3389/FMED.2021.615978>.
- [6] Li, Y., Fan, W., Link, F., Wang, S., Dooley, S., 2021. Transforming growth factor  $\beta$  latency: a mechanism of cytokine storage and signalling regulation in liver homeostasis and disease. *JHEP Reports: Innovation in Hepatology* 4(2). <https://doi.org/10.1016/J.JHEPR.2021.100397>.
- [7] Tan, Z., Qian, X., Jiang, R., Liu, Q., Wang, Y., Chen, C., et al., 2013. IL-17A plays a critical role in the pathogenesis of liver fibrosis through hepatic stellate cell activation. *The Journal of Immunology* 191(4):1835–1844. <https://doi.org/10.4049/JIMMUNOL.1203013>.
- [8] Xu, F., Liu, C., Zhou, D., Zhang, L., 2016. TGF- $\beta$ /SMAD pathway and its regulation in hepatic fibrosis. *Journal of Histochemistry and Cytochemistry: Official Journal of the Histochemistry Society* 64(3):157–167. <https://doi.org/10.1369/0022155415627681>.
- [9] Sun, Y.Y., Li, X.F., Meng, X.M., Huang, C., Zhang, L., Li, J., 2017. Macrophage phenotype in liver injury and repair. *Scandinavian Journal of Immunology* 85(3):166–174. <https://doi.org/10.1111/SJ.12468>.
- [10] Magee, N., Zou, A., Zhang, Y., 2016. Pathogenesis of nonalcoholic steatohepatitis: interactions between liver parenchymal and nonparenchymal cells. *BioMed Research International* 2016. <https://doi.org/10.1155/2016/5170402>.
- [11] Higashi, T., Friedman, S.L., Hoshida, Y., 2017. Hepatic stellate cells as key target in liver fibrosis. *Advanced Drug Delivery Reviews* 121:27–42. <https://doi.org/10.1016/J.ADDR.2017.05.007>.
- [12] Lonardo, A., Nascimben, F., Ballestri, S., Fairweather, D.L., Win, S., Than, T.A., et al., 2019. Sex differences in nonalcoholic fatty liver disease: state of the art and identification of research gaps, vol. 70. *Hepatology*. p. 1457–69.
- [13] Chanbin, L., Kim, J., Jung, Y., 2019. Potential therapeutic application of estrogen in gender disparity of nonalcoholic fatty liver disease/nonalcoholic steatohepatitis. *Cells* 8(10). <https://doi.org/10.3390/CELLS8101259>.
- [14] DiStefano, J.K., 2020. NAFLD and NASH in postmenopausal women: implications for diagnosis and treatment. *Endocrinology*, 1–12. <https://doi.org/10.1210/endo/bqaa134>.
- [15] Ponnusamy, S., Tran, Q.T., Thiyagarajan, T., Miller, D.D., Bridges, D., Narayanan, R., 2017. An estrogen receptor  $\beta$ -selective agonist inhibits non-alcoholic steatohepatitis in preclinical models by regulating bile acid and xenobiotic receptors. *Experimental Biology and Medicine* 242(6):606–616. <https://doi.org/10.1177/1535370216688569>.
- [16] Zhang, B., Zhang, C.G., Ji, L.H., Zhao, G., Wu, Z.Y., 2018. Estrogen receptor  $\beta$  selective agonist ameliorates liver cirrhosis in rats by inhibiting the activation and proliferation of hepatic stellate cells. *Journal of Gastroenterology and Hepatology* 33(3):747–755. <https://doi.org/10.1111/jgh.13976>.
- [17] Zhang, C.G., Zhang, B., Deng, W.S., Duan, M., Chen, W., Wu, Z.Y., 2016. Role of estrogen receptor  $\beta$  selective agonist in ameliorating portal hypertension in rats with CCl<sub>4</sub>-induced liver cirrhosis. *World Journal of Gastroenterology* 22(18):4484–4500. <https://doi.org/10.3748/wjg.v22.i18.4484>.

- [18] Cortes, E., Lachowski, D., Rice, A., Thorpe, S.D., Robinson, B., Yeldag, G., et al., 2019. Tamoxifen mechanically deactivates hepatic stellate cells via the G protein-coupled estrogen receptor. *Oncogene*. <https://doi.org/10.1038/s41388-018-0631-3>.
- [19] Zhang, B., Wu, Z., 2013. Estrogen derivatives: novel therapeutic agents for liver cirrhosis and portal hypertension. *European Journal of Gastroenterology and Hepatology* 25(3):263–270. <https://doi.org/10.1097/MEG.0B013E32835AB5DC>.
- [20] Guo, S., Yu, Y., Zhang, N., Cui, Y., Zhai, L., Li, H., et al., 2014. Higher level of plasma bioactive molecule sphingosine 1-phosphate in women is associated with estrogen. *Biochimica et Biophysica Acta* 1841(6):836–846. <https://doi.org/10.1016/j.bbali.2014.02.005>.
- [21] Yasuda, M., Shimizu, I., Shiba, M., Ito, S., 1999. Suppressive effects of estradiol on dimethylnitrosamine-induced fibrosis of the liver in rats. *Hepatology* 29(3):719–727. <https://doi.org/10.1002/HEP.510290307>.
- [22] Stapelfeld, C., Dammann, C., Maser, E., 2020. Sex-specificity in lung cancer risk. *International Journal of Cancer*, 2376–2382. <https://doi.org/10.1002/ijc.32716>.
- [23] Tian, G.X., Sun, Y., Pang, C.J., Tan, A.H., Gao, Y., Zhang, H.Y., et al., 2012. Oestradiol is a protective factor for non-alcoholic fatty liver disease in healthy men. *Obesity Reviews: An Official Journal of the International Association for the Study of Obesity* 13(4):381–387. <https://doi.org/10.1111/J.1467-789X.2011.00978.X>.
- [24] Yang, L., Weng, W., Sun, Z.X., Fu, X.J., Ma, J., Zhuang, W.F., 2015. SphK1 inhibitor II (SKI-II) inhibits acute myelogenous leukemia cell growth in vitro and in vivo. *Biochemical and Biophysical Research Communications* 460(4):903–908. <https://doi.org/10.1016/j.bbrc.2015.03.114>.
- [25] Simon, J., Ouro, A., Ala-Ibanibo, L., Presa, N., Delgado, T.C., Martínez-Chantar, M.L., 2020. Sphingolipids in non-alcoholic fatty liver disease and hepatocellular carcinoma: ceramide turnover. *International Journal of Molecular Sciences*. <https://doi.org/10.3390/ijms21010040>.
- [26] Ishay, Y., Nachman, D., Khoury, T., Ilan, Y., 2020. The role of the sphingolipid pathway in liver fibrosis: an emerging new potential target for novel therapies. *American Journal of Physiology – Cell Physiology* 318(6):C1055–C1064. <https://doi.org/10.1152/AJPCELL.00003.2020>.
- [27] Zhang, X., Ritter, J.K., Li, N., 2018. Sphingosine-1-phosphate pathway in renal fibrosis. *American Journal of Physiology – Renal Physiology* 315(4):F752–F756. <https://doi.org/10.1152/AJPRENAL.00596.2017>.
- [28] Hajny, S., Christoffersen, C., 2017. A novel perspective on the ApoM-S1P axis, highlighting the metabolism of ApoM and its role in liver fibrosis and neuroinflammation. *International Journal of Molecular Sciences* 18(8). <https://doi.org/10.3390/IJMS18081636>.
- [29] Zheng, Z., Ma, T., Guo, H., Kim, K.S., Kim, K.T., Bi, L., et al., 2019. 4-O-Methylhonokiol protects against diabetic cardiomyopathy in type 2 diabetic mice by activation of AMPK-mediated cardiac lipid metabolism improvement. *Journal of Cellular and Molecular Medicine* 23(8):5771–5781. <https://doi.org/10.1111/JCMM.14493>.
- [30] Ma, T., Zheng, Z., Guo, H., Lian, X., Rane, M., Cai, L., et al., 2019. 4-O-Methylhonokiol ameliorates type 2 diabetes-induced nephropathy in mice likely by activation of AMPK-mediated fatty acid oxidation and Nrf2-mediated anti-oxidative stress. *Toxicology and Applied Pharmacology* 370:93–105. <https://doi.org/10.1016/j.taap.2019.03.007>.
- [31] Russo, S.B., Baicu, C.F., Van Laer, A., Geng, T., Kasiganesan, H., Zile, M.R., et al., 2012. Ceramide synthase 5 mediates lipid-induced autophagy and hypertrophy in cardiomyocytes. *Journal of Clinical Investigation* 122(11):3919–3930. <https://doi.org/10.1172/JCI63888>.
- [32] Russo, S.B., Tidhar, R., Futerman, A.H., Cowart, L.A., 2013. Myristate-derived d16:0 sphingolipids constitute a cardiac sphingolipid pool with distinct synthetic routes and functional properties. *Journal of Biological Chemistry* 288(19):13397–13409. <https://doi.org/10.1074/jbc.M112.428185>.
- [33] Geng, T., Hu, W., Broadwater, M.H., Snider, J.M., Bielawski, J., Russo, S.B., et al., 2013. Fatty acids differentially regulate insulin resistance through endoplasmic reticulum stress-mediated induction of tribbles homologue 3: a potential link between dietary fat composition and the pathophysiological outcomes of obesity. *Diabetologia* 56(9):2078–2087. <https://doi.org/10.1007/s00125-013-2973-2>.
- [34] Choi, S., Snider, J.M., Cariello, C.P., Lambert, J.M., Anderson, A.K., Cowart, L.A., et al., 2020. Sphingosine kinase 1 is required for myristate-induced TNF $\alpha$  expression in intestinal epithelial cells. *Prostaglandins & Other Lipid Mediators* 149:106423. <https://doi.org/10.1016/j.prostaglandins.2020.106423>.
- [35] Sutter, A.G., Palanisamy, A.P., Lench, J.H., Eskilsen, S., Geng, T., Lewin, D.N.B., et al., 2016. Dietary saturated fat promotes development of hepatic inflammation through toll-like receptor 4 in mice. *Journal of Cellular Biochemistry* 117(7):1613–1621. <https://doi.org/10.1002/JCB.25453>.
- [36] Geng, T., Sutter, A., Harland, M.D., Law, B.A., Ross, J.S., Lewin, D., et al., 2015. SphK1 mediates hepatic inflammation in a mouse model of NASH induced by high saturated fat feeding and initiates proinflammatory signaling in hepatocytes. *The Journal of Lipid Research* 56(12):2359–2371. <https://doi.org/10.1194/jlr.M063511>.
- [37] Maceyka, M., Harikumar, K.B., Milstien, S., Spiegel, S., 2012. Sphingosine-1-phosphate signaling and its role in disease. *Trends in Cell Biology* 22(1):50–60. <https://doi.org/10.1016/j.tcb.2011.09.003>.
- [38] Kunkel, G.T., Maceyka, M., Milstien, S., S.S., 2013. Targeting the sphingosine-1-phosphate axis in cancer, inflammation and beyond. *Nature Reviews Drug Discovery* 12(9):688–702. <https://doi.org/10.1038/NRD4099>.
- [39] Maceyka, M., Spiegel, S., 2014. Sphingolipid metabolites in inflammatory disease. *Nature* 510(7503):58–67. <https://doi.org/10.1038/NATURE13475>.
- [40] King, A., Houlihan, D.D., Kavanagh, D., Haldar, D., Luu, N., Owen, A., et al., 2017. Sphingosine-1-phosphate prevents egress of hematopoietic stem cells from liver to reduce fibrosis. *Gastroenterology* 153(1). <https://doi.org/10.1053/J.GASTRO.2017.03.022>, 233–248.e16.
- [41] Pappu, R., Schwab, S.R., Cornelissen, I., Pereira, J.P., Regard, J.B., Xu, Y., et al., 2007. Promotion of lymphocyte egress into blood and lymph by distinct sources of sphingosine-1-phosphate. *Science* 316(5822):295–298. <https://doi.org/10.1126/SCIENCE.1139221>.
- [42] Postic, C., Shiota, M., Niswender, K.D., Jetton, T.L., Chen, Y., Moates, J.M., et al., 1999. Dual roles for glucokinase in glucose homeostasis as determined by liver and pancreatic beta cell-specific gene knock-outs using Cre recombinase. *Journal of Biological Chemistry* 274(1):305–315. <https://doi.org/10.1074/JBC.274.1.305>.
- [43] Arnesano, C., Santoro, Y., Gratton, E., 2012. Digital parallel frequency-domain spectroscopy for tissue imaging. *Journal of Biomedical Optics* 17(9):0960141. <https://doi.org/10.1117/1.JBO.17.9.096014>.
- [44] Ranjit, S., Dobrinskikh, E., Montford, J., Dvornikov, A., Lehman, A., Orlicky, D.J., et al., 2016. Label-free fluorescence lifetime and second harmonic generation imaging microscopy improves quantification of experimental renal fibrosis. *Kidney International* 90(5):1123–1128. <https://doi.org/10.1016/j.kint.2016.06.030>.
- [45] Malacrida, L., Ranjit, S., Jameson, D.E., Gratton, E., 2021. The phasor plot: a universal circle to advance fluorescence lifetime analysis and interpretation. *Annual Review of Biophysics* 50:575–593. <https://doi.org/10.1146/ANNUREV-BIOPHYS-062920-063631>.
- [46] Ranjit, S., Malacrida, L., Jameson, D.M., Gratton, E., 2018. Fit-free analysis of fluorescence lifetime imaging data using the phasor approach. *Nature Protocols* 13(9):1979–2004. <https://doi.org/10.1038/S41596-018-0026-5>.
- [47] Seglen, P.O., 1976. Preparation of isolated rat liver cells. *Methods in Cell Biology* 13(C):29–83. [https://doi.org/10.1016/S0091-679X\(08\)61797-5](https://doi.org/10.1016/S0091-679X(08)61797-5).
- [48] Qiu, B., Wei, F., Sun, X., Wang, X., Duan, B., Shi, C., et al., 2014. Measurement of hydroxyproline in collagen with three different methods.

- Molecular Medicine Reports 10(2):1157–1163. <https://doi.org/10.3892/MMR.2014.2267>.
- [49] Maczisz, M.A., Maceyka, M., Waters, M.R., Newton, J., Singh, M., Rigsby, M.F., et al., 2018. Sphingosine kinase 1 activation by estrogen receptor  $\alpha$ 36 contributes to tamoxifen resistance in breast cancer. *Journal of Lipid Research* 59(12):2297–2307. <https://doi.org/10.1194/JLR.M085191>.
- [50] Postic, C., Magnuson, M.A., 2000. DNA excision in liver by an albumin-Cre transgene occurs progressively with age. *Genesis* 26(2):149–150. [https://doi.org/10.1002/\(sici\)1526-968x\(200002\)26:2<149::aid-gene16>3.0.co;2-v](https://doi.org/10.1002/(sici)1526-968x(200002)26:2<149::aid-gene16>3.0.co;2-v).
- [51] Huang, D.Q., El-Serag, H.B., Loomba, R., 2021. Global epidemiology of NAFLD-related HCC: trends, predictions, risk factors and prevention. *Nature Reviews Gastroenterology & Hepatology* 18(4):223–238. <https://doi.org/10.1038/S41575-020-00381-6>.
- [52] Kim, B.M., Abdelfattah, A.M., Vasan, R., Fuchs, B.C., Choi, M.Y., 2018. Hepatic stellate cells secrete Ccl5 to induce hepatocyte steatosis. *Scientific Reports* 8(1). <https://doi.org/10.1038/S41598-018-25699-9>.
- [53] Campagnola, P., 2011. Second harmonic generation imaging microscopy: applications to diseases diagnostics. *Analytical Chemistry* 83(9):3224–3231. <https://doi.org/10.1021/AC1032325>.
- [54] Ranjit, S., Dvornikov, A., Stakic, M., Hong, S.H., Levi, M., Evans, R.M., et al., 2015. Imaging fibrosis and separating collagens using second harmonic generation and phasor approach to fluorescence lifetime imaging. *Scientific Reports* 5. <https://doi.org/10.1038/SREP13378>.
- [55] Bedossa, P., Poynard, T., 1996. An algorithm for the grading of activity in chronic hepatitis C. The METAVIR Cooperative Study Group. *Hepatology* 24(2): 289–293. <https://doi.org/10.1002/HEP.510240201>.
- [56] Gailhouste, L., Le Grand, Y., Odin, C., Guyader, D., Turlin, B., Ezan, F., et al., 2010. Fibrillar collagen scoring by second harmonic microscopy: a new tool in the assessment of liver fibrosis. *Journal of Hepatology* 52(3):398–406. <https://doi.org/10.1016/J.JHEP.2009.12.009>.
- [57] Deng, Q., Clemas, J.A., Chrebet, G., Fischer, P., Hale, J.J., Li, Z., et al., 2007. Identification of Leu276 of the S1P1 receptor and Phe263 of the S1P3 receptor in interaction with receptor specific agonists by molecular modeling, site-directed mutagenesis, and affinity studies. *Molecular Pharmacology* 71(3): 724–735. <https://doi.org/10.1124/MOL.106.029223>.
- [58] Sukocheva, O.A., Wang, L., Albanese, N., Pitson, S.M., Vadas, M.A., Xia, P., 2003. Sphingosine kinase transmits estrogen signaling in human breast cancer cells. *Molecular Endocrinology* 17(10):2002–2012. <https://doi.org/10.1210/ME.2003-0119>.
- [59] Que, R., Shen, Y., Ren, J., Tao, Z., Zhu, X., Li, Y., 2018. Estrogen receptor- $\beta$ -dependent effects of saikosaponin-d on the suppression of oxidative stress-induced rat hepatic stellate cell activation. *International Journal of Molecular Medicine* 41(3):1357–1364. <https://doi.org/10.3892/IJMM.2017.3349>.
- [60] Surico, D., Ercoli, A., Farruggio, S., Raina, G., Filippini, D., Mary, D., et al., 2017. Modulation of oxidative stress by 17  $\beta$ -estradiol and genistein in human hepatic cell lines in vitro. *Cellular Physiology and Biochemistry: International Journal of Experimental Cellular Physiology, Biochemistry, and Pharmacology* 42(3):1051–1062. <https://doi.org/10.1159/000478752>.
- [61] Itagaki, T., Shimizu, I., Cheng, X., Yuan, Y., Oshio, A., Tamaki, K., et al., 2005. Opposing effects of oestradiol and progesterone on intracellular pathways and activation processes in the oxidative stress induced activation of cultured rat hepatic stellate cells. *Gut* 54(12):1782–1789. <https://doi.org/10.1136/GUT.2005.053278>.
- [62] Wang, E., He, X., Zeng, M., 2019. The role of S1P and the related signaling pathway in the development of tissue fibrosis. *Frontiers in Pharmacology* 9(JAN). <https://doi.org/10.3389/FPHAR.2018.01504>.
- [63] Yang, L., Yue, S., Yang, L., Liu, X., Han, Z., Zhang, Y., et al., 2013. Sphingosine kinase/sphingosine 1-phosphate (S1P)/S1P receptor axis is involved in liver fibrosis-associated angiogenesis. *Journal of Hepatology* 59(1):114–123. <https://doi.org/10.1016/J.JHEP.2013.02.021>.
- [64] Li, Q.F., Wu, C.T., Duan, H.F., Sun, H.Y., Wang, H., Lu, Z.Z., et al., 2007. Activation of sphingosine kinase mediates suppressive effect of interleukin-6 on human multiple myeloma cell apoptosis. *British Journal of Haematology* 138(5):632–639. <https://doi.org/10.1111/J.1365-2141.2007.06711.X>.
- [65] Li, C., Kong, Y., Wang, H., 2009. Homing of bone marrow mesenchymal stem cells mediated by sphingosine 1-phosphate contributes to liver fibrosis. *Journal of Hepatology* 50(6):1174–1183. <https://doi.org/10.1016/J.JHEP.2009.01.028>.
- [66] Wang, Y., Aoki, H., Yang, J., Peng, K., Liu, R., Li, X., et al., 2017. The role of sphingosine 1-phosphate receptor 2 in bile-acid-induced cholangiocyte proliferation and cholestasis-induced liver injury in mice. *Hepatology* 65(6):2005–2018. <https://doi.org/10.1002/HEP.29076>.
- [67] Ikeda, H., Watanabe, N., Ishii, I., Shimosawa, T., Kume, Y., Tomiya, T., et al., 2009. Sphingosine 1-phosphate regulates regeneration and fibrosis after liver injury via sphingosine 1-phosphate receptor 2. *Journal of Lipid Research* 50(3):556–564.
- [68] Kong, Y., Wang, H., Wang, S., Tang, N., 2014. FTY720, a sphingosine-1 phosphate receptor modulator, improves liver fibrosis in a mouse model by impairing the motility of bone marrow-derived mesenchymal stem cells. *Inflammation* 37(4):1326–1336. <https://doi.org/10.1007/S10753-014-9877-2>.
- [69] Yang, L., Han, Z., Tian, L., Mai, P., Zhang, Y., Wang, L., et al., 2015. Sphingosine 1-phosphate receptor 2 and 3 mediate bone marrow-derived monocyte/macrophage motility in cholestatic liver injury in mice. *Scientific Reports* 5. <https://doi.org/10.1038/SREP13423>.
- [70] Kageyama, Y., Ikeda, H., Watanabe, N., Nagamine, M., Kusumoto, Y., Yashiro, M., et al., 2012. Antagonism of sphingosine 1-phosphate receptor 2 causes a selective reduction of portal vein pressure in bile duct-ligated rodents. *Hepatology* 56(4):1427–1438. <https://doi.org/10.1002/HEP.25780>.
- [71] Ding, B.S., Liu, C., Sun, Y., Chen, Y., Swendeman, S., Jung, B., et al., 2016. HDL activation of endothelial sphingosine-1-phosphate receptor-1 (S1P 1) promotes regeneration and suppresses fibrosis in the liver. *JCI Insight* 1(21). <https://doi.org/10.1172/JCI.INSIGHT.87058>.
- [72] Ge, J., Chang, N., Zhao, Z., Tian, L., Duan, X., Yang, L., et al., 2016. Essential roles of RNA-binding protein HuR in activation of hepatic stellate cells induced by transforming growth factor- $\beta$ 1. *Scientific Reports* 6. <https://doi.org/10.1038/SREP22141>.
- [73] González-Fernández, B., Sánchez, D.I., González-Gallego, J., Tuñón, M.J., 2017. Sphingosine 1-phosphate signaling as a target in hepatic fibrosis therapy. *Frontiers in Pharmacology* 8(AUG). <https://doi.org/10.3389/FPHAR.2017.00579>.
- [74] Brunati, A.M., Tibaldi, E., Carraro, A., Gringer, E., D’Amico, F., Toninello, A., et al., 2008. Cross-talk between PDGF and S1P signalling elucidates the inhibitory effect and potential antifibrotic action of the immunomodulator FTY720 in activated HSC-cultures. *Biochimica et Biophysica Acta* 1783(3): 347–359. <https://doi.org/10.1016/J.BBAMCR.2007.11.008>.
- [75] Yang, L., Chang, N., Liu, X., Han, Z., Zhu, T., Li, C., et al., 2012. Bone marrow-derived mesenchymal stem cells differentiate to hepatic myofibroblasts by transforming growth factor- $\beta$ 1 via sphingosine kinase/sphingosine 1-phosphate (S1P)/S1P receptor axis. *American Journal of Pathology* 181(1): 85–97. <https://doi.org/10.1016/J.AJP.2012.03.014>.
- [76] Xiu, L., Chang, N., Yang, L., Liu, X., Yang, L., Ge, J., et al., 2015. Intracellular sphingosine 1-phosphate contributes to collagen expression of hepatic myofibroblasts in human liver fibrosis independent of its receptors. *American Journal of Pathology* 185(2):387–398. <https://doi.org/10.1016/J.AJP.2014.09.023>.
- [77] Alshaker, H., Thrower, H., Pchejetski, D., 2020. Sphingosine kinase 1 in breast cancer — a new molecular marker and a therapy target. *Frontiers in Oncology* 10:289. <https://doi.org/10.3389/FONC.2020.00289>.
- [78] Wei, J., Shi, Y., Zhang, X., Feng, Y., Luo, G., Zhang, J., et al., 2011. Estrogen upregulates hepatic apolipoprotein M expression via the estrogen receptor.

- Biochimica et Biophysica Acta 1811(12):1146–1151. <https://doi.org/10.1016/J.BBALIP.2011.07.003>.
- [79] Kurano, M., Tsukamoto, K., Ohkawa, R., Hara, M., Iino, J., Kageyama, Y., et al., 2013. Liver involvement in sphingosine 1-phosphate dynamism revealed by adenoviral hepatic overexpression of apolipoprotein M. *Atherosclerosis* 229(1):102–109. <https://doi.org/10.1016/j.atherosclerosis.2013.04.024>.
- [80] Wilkerson, B.A., Grass, D.B., Wing, S.B., Argraves, W.S., Argraves, K.M., 2012. Sphingosine 1-phosphate (S1P) carrier-dependent regulation of endothelial barrier: high density lipoprotein (HDL)-S1P prolongs endothelial barrier enhancement as compared with albumin-S1P via effects on levels, trafficking, and signaling of S1P1. *Journal of Biological Chemistry* 287(53):44645–44653. <https://doi.org/10.1074/JBC.M112.423426>.
- [81] Galvani, S., Sanson, M., Blaho, V.A., Swendeman, S.L., Obinata, H., Conger, H., et al., 2015. HDL-bound sphingosine 1-phosphate acts as a biased agonist for the endothelial cell receptor S1P1 to limit vascular inflammation. *Science Signaling* 8(389). <https://doi.org/10.1126/SCISIGNAL.AAA2581>.